Energy Conversion and Management: X 22 (2024) 100561

Contents lists available at ScienceDirect

Energy Conversion and Management: X

journal homepage: www.sciencedirect.com/journal/energy-conversion-and-management-x

Closed loop model predictive control of a hybrid battery-hydrogen energy storage system using mixed-integer linear programming

Alexander Holtwerth [a,*], André Xhonneux [a], Dirk Müller [a,b]

[a] Institute of Energy and Climate Research – Energy Systems Engineering (IEK-10), Forschungszentrum Jülich GmbH, Wilhelm-Johnen-Straße, Jülich 52428, Germany
[b] Institute for Energy Efficient Buildings and Indoor Climate, E.ON Energy Research Center, RWTH Aachen University, Mathieustraße 10, Aachen 52074, Germany

ARTICLE INFO

Keywords:
Model predictive control
Optimization
Mixed integer linear programming
Hybrid battery-hydrogen energy storage system

ABSTRACT

The derivation of an efficient operational strategy for storing intermittent renewable energies using a hybrid battery-hydrogen energy storage system is a difficult task. One approach for deriving an efficient operational strategy is using mathematical optimization in the context of model predictive control. However, mathematical optimization derives an operational strategy based on a non-exact mathematical system representation for a specified prediction horizon to optimize a specified target. Thus, the resulting operational strategies can vary depending on the optimization settings.

This work focuses on evaluating potential improvements in the operational strategy for a hybrid battery-hydrogen energy storage system using mathematical optimization. To investigate the operation, a simulation model of a hybrid energy storage system and a tailor-made mixed integer linear programming optimization model of this specific system are utilized in the context of a model predictive control framework. The resulting operational strategies for different settings of the model predictive control framework are compared to a rule-based controller to show the potential benefits of model predictive control compared to a conventional approach. Furthermore, an in-depth analysis of different factors that impact the effectiveness of the model predictive controller is done. Therefore, a sensitivity analysis of the effect of different electricity demands and resource sizes on the performance relative to a rule-based controller is conducted. The model predictive controller reduced the energy consumption by at least 3.9 % and up to 17.9% compared to a rule-based controller. Finally, Pareto fronts for multi-objective optimizations with different prediction and control horizons are derived and compared to the results of a rule-based controller. A cost reduction of up to 47 % is achieved by a model predictive controller with a prediction horizon of 7 days and perfect foresight.

1. Introduction

In recent years, the share of renewable energies in the German energy mix has been increasing to reduce the emission of greenhouse gasses. Especially the share of renewable energies from solar and wind has been increasing recently [1]. However, the electricity produced by solar and wind power plants is highly volatile [2] due to the high dependency on environmental conditions. To achieve independence from fossil energy sources, decentralized energy storage systems can be utilized to mitigate the intermittent nature of renewable energy generation on the scale of minutes up to seasonal variations in energy availability [3]. Thus, efficient large-scale storage solutions are needed to cope with this large variety of different time scales on which the fluctuations in energy production occur [4]. Hybrid energy storage systems can lead to a cost-effective tradeoff between highly efficient short-term energy storage using battery storage systems (BSS) and cost-effective large-scale, long-term energy storage using hydrogen storage systems (HSS) [5].

The chosen energy management strategy (EMS) is essential for the longevity and efficiency of hybrid energy systems [6]. Therefore, many different energy management strategies have been proposed in the literature. A review of different control algorithms was done by Van et al. [7]. Model predictive control (MPC) is one approach widely adopted in literature as it provides the possibility of combining forecasts regarding the energy price, the available resources, and the demands to derive an optimal schedule for the energy system [8].

The optimal scheduling of hybrid battery-hydrogen energy storage systems has been an active field of research for many years now. In 2003

* Corresponding author.
E-mail address: a.holtwerth@fz-juelich.de (A. Holtwerth).

https://doi.org/10.1016/j.ecmx.2024.100561

Available online 9 March 2024

Korpaas et al.[9] incorporated a hydrogen storage system in a system with an intermittent stochastic energy source and an uncertain energy demand, showing the benefits of utilizing mathematical optimization to derive the operational strategy. Cau et al. [10] investigated the impact of mathematical optimization compared to a rule-based operation of a hybrid energy system using a mixed integer linear programming (MILP) formulation in 2014, revealing the potential of utilizing mathematical optimization with a cost reduction of about 15 %. In 2015, Valverde et al. [11] experimentally validated their model predictive controller and compared the derived operational strategy to a rule-based controller (RBC), showing a 30% reduction in operational cost in a real-world experiment. More recently, Daneshvar et al. [12] derived an MPC using the market participation of hydrogen energy storages in a day-ahead market. Gbadega et al. [13] investigated the impact of incorporating disturbance prediction on the performance of an EMS using an adaptive MPC to reduce the operating cost of a hybrid-energy storage system. Furthermore, Huang et al. [14] developed an economic model predictive controller with a scheduling correction algorithm to achieve a tradeoff between the computational time and the scheduling accuracy.

Besides the advances in MPC, RBC remains the prevalent energy management strategy in practical applications for renewable energy systems with hydrogen storage [15], due to the simplicity of RBC and relative ease of implementation [16]. Thus, RBCs are used in recent literature to control hydrogen energy storage systems. Le et al. [5] utilized a rule-based controller as EMS in their study on the optimal sizing of a hybrid energy storage system. Similarly, Modu et al. [17] utilized a rule-based EMS for their hybrid renewable energy storage system to manage the power flow of their components. Furthermore, Li et al. [18] utilized a hysteresis band-based power management strategy in their multi-objective objective optimization approach to determine the optimal system size. Moreover, Šimunović et al. [19] utilized several rule-based algorithms as EMS to investigate the effect of capacity losses on the performance of stand-alone hybrid battery-hydrogen energy storage systems. A techno-economic assessment of integrating hydrogen energy storage was done by Alili et al. [20] using a rule-bases EMS.

Hence, RBCs are still used as a benchmark to show the performance increases to be gained from utilizing mathematical optimization to derive the optimal operational strategy. Clarke et al. [21] compared their two-layer economic model predictive controller to a conventional rule-based controller and found that the operating cost and the CO_2 emissions can be decreased by 5–10% utilizing model predictive control. Gonzalez-Rivera et al. [22] benchmarked their model predictive controller for the operation of a hybrid charging station against a rule-based controller. The model predictive controller was found to reduce the utilization cost by 25.3%. In 2021, Yamashita et al. [23] achieved a 5% to 9% decreased operation cost utilizing their two-level hierarchal model predictive controller in comparison to an RBC. Li et al. [24] compared their power management approach based on game theory for a hybrid battery-hydrogen energy system with a model predictive controller and a rule-based controller. Kumar et al. [25] utilized a rule-based controller and a model predictive controller as benchmarks for their two-layer EMS with a fuzzy control logic in a supervisory layer. Furthermore, in 2023, Thaler et al. [26] showed that by utilizing MPC, the system size could be reduced by 12% in comparison to an RBC while fulfilling the system requirements. However, to the best of the author's knowledge, no extensive investigations on factors such as energy availability, the season, or additional boundary conditions impacting the performance of MPC in comparison to RBC exist.

Furthermore, the prediction horizon, as well as the control horizon chosen for the MPC, are generally considered to be constant in the literature. As stated by Shahzad et al. [27], long-prediction horizons pose a challenge for the MPC technique because longer prediction horizons might increase the computational complexity. Therefore, most MPC approaches utilize a prediction horizon of 24 h or less. For instance, Garcia-Torres et al. [28] derived a hierarchical model predictive controller to optimize the operation of a hybrid energy system with a prediction horizon of up to 24 h. Valverde et al. [11] optimized the operation of a real-world hybrid energy system using a prediction horizon of 10 h. Even though the computational resources have been increasing for the past decades [29], recent studies still utilize a short prediction horizon. Abdelghany et al. [30] utilized a prediction horizon of 24 h to optimize the operation of a hydrogen-based energy storage system. Similarly, Abdelghany et al. [31] utilized a prediction horizon of 24 h in their stochastic model predictive controller while stating that a longer prediction horizon would be feasible. In a recent work, Abdelghany et al. [8] developed a hierarchical model predictive controller with a prediction horizon of 24 h in the high-level controller. Similarly, Shen et al. [32] developed a multi-time scale rolling horizon optimization approach for a hybrid energy storage system while considering a prediction horizon of 24 h. Furthermore, in a recent study, Thaler et al. [26] utilized an MPC approach with a prediction horizon of 24 h while adding additional terms to the cost function to incentivize energy storage. However, Thaler et al. [26] state that more efficient thermal energy storage should be achievable with longer prediction horizons. Cardona et al. [33] showed that utilizing long prediction horizons of up to 7 days increases the performance of their MPC approach for an on-site green hydrogen production and refueling station, showing that the consideration of long prediction horizons can increase the system performance. To the best of the author's knowledge, for grid-connected hybrid battery-hydrogen energy storage systems, no extensive studies exist focusing on the impact of a varying prediction horizon length, a varying control horizon length, and a varying price prediction horizon length on Pareto optimal solutions of an MPC framework utilizing multi-objective optimizations.

This work's contribution is an extensive investigation of the impact of different settings influencing the performance of an MPC. Therefore, a detailed mixed integer linear programming (MILP) optimization model is derived using a data-driven modeling approach that makes use of open-source simulation models of the components of the energy storage system. The resulting operational strategies of the MPC are validated by a simulation model derived in Modelica and compared to the operation derived by a classical RBC.

First, this work thoroughly analyses the impact of different external conditions, like the impact of seasonal availability of solar energy on the performance of an MPC compared to an RBC. Furthermore, the impact of different demand and resource sizes and boundary conditions on the performance of the MPC compared to an RBC is investigated. This investigation is carried out by simulating the yearly energy consumption of the energy system for 27 different settings for each controller. The second contribution is an extensive investigation of the potential benefits gained from utilizing long prediction horizons in the optimization problem to control the hybrid battery-hydrogen energy storage system. This is done by deriving multiple Pareto fronts for multi-objective optimizations to minimize electricity consumption and operational costs. Therefore, the yearly energy consumption for 102 different settings in the MPC framework is evaluated. Such extensive investigations using a simulation model as a substitute for the real-world system can help identify the most critical influencing factors for the selected model predictive control approach before utilizing it on the real-world system. Thus, this study shows a comprehensive overview of the factors impacting the performance of a model predictive controller. The key aspects of this work are the following:

- Derivation of a MILP optimization model making use of a Modelica simulation model
- Utilization of the optimization model for MPC of the hybrid battery-hydrogen energy storage system via an MPC framework
- Sensitivity analysis of the performance of an MPC in comparison to an RBC
- Investigation of the impact of different modeling parameters on the effectiveness of the MPC

- Analysis of the influence of the control and prediction horizon on the Pareto optimal solutions for a multi-objective cost and energy consumption minimization

The sections of this work are ordered as follows: The simulation and optimization model, as well as the MPC framework, are described in Section 2. Section 3 describes the conducted case studies. The results of the case study are shown in Section 4. Finally, Section 5 discusses the results and draws a conclusion.

2. Methods

The following section describes the simulation model in 2.1. For the optimization problem, the nonlinear operational behavior of the fuel cell, electrolyzer, and compressor are modeled as piecewise linear functions using the modeling toolbox LinMOG as described in Section 2.2. The optimization problem is derived in Section 2.3. Finally, the interaction between the simulation model of the whole energy system and the optimization problem in the scope of the model predictive control framework is described in 2.4.

2.1. Simulation model

The energy system consists of a PV park for generating renewable energy, an electricity demand that needs to be fulfilled, a BSS for efficient short-term storage, and an HSS for long-term energy storage. Furthermore, the energy system is connected to the electrical grid, so electrical energy is always available. A local grid connects all components and all consumers. The local grid is modeled as an ideal conductor such that no transmission losses occur. A sketch of the energy system is shown in Fig. 1.

The simulation model is derived using the modeling language Modelica to enable the utilization of open-source component models developed in the literature. The utilized electrolyzer and fuel cell models are based on the models developed in the TransiEnt library [34]. The electrolyzer model is based on experimental data as explained in [35], while the fuel cell stack model is based on a detailed simulation model, including a pressure and temperature model. The models selected in this work approximate the hydrogen consumption and production of the fuel cell and the electrolyzer. The simulated hydrogen output of the electrolyzer $n^{\mathrm{H2,ey}}$ as a function of the power input p^{ey} is shown in Fig. 2 (a). The hydrogen consumption of the fuel cell $n^{\mathrm{H2,fc}}$ as a function of the electricity output p^{fc} is shown in Fig. 2 (b). The electrolyzer model achieves an efficiency of 63 % based on the lower heating value of hydrogen LHV $= 241.818$ kJ/mol, which is similar to values reported in literature [36]. Furthermore, the fuel cell model achieves an efficiency of 50 % based on the LHV, which is similar to values reported in literature [37]. The inlet pressure of the fuel cell is lowered from the variable pressure of the storage pressure system to a constant pressure of 1.5 bar.

The battery model of the buildings library [38] is used with a capacity of $C^{\mathrm{bat}} = 600$ kWh and a maximal electricity charging and discharging power of $p^{\mathrm{bat,max,el}} = 100$ kW. The battery charging and discharging efficiency is 90 %, and no self-discharge or aging effects are considered. Additional components, such as the pressure storage tank and the compressor, are modeled using typical approaches from literature, such as the ideal gas law and the specific work for isentropic compression [39]. Thus, a change in the storage pressure pr^{ps} is calculated by:

$$\Delta pr^{\mathrm{ps}} = \frac{(n^{\mathrm{H2,comp}} - n^{\mathrm{H2,fc}}) \cdot R \cdot T^{\mathrm{ps}}}{V^{\mathrm{ps}}} \Delta t \tag{1}$$

where R is the universal gas constant, $T^{\mathrm{ps}} = 293.15$ K is temperature, $V^{\mathrm{ps}} = 30.238$ m^3 is the volume of the pressure storag tank, and Δt is the time step width. The minimal storage pressure $pr^{\mathrm{ps,min}}$ is 5 bar, and the maximal storage pressure $pr^{\mathrm{ps,max}}$ is 50 bar. If the maximal pressure of 50 bar within the pressure storage is exceeded, a valve vents the excess hydrogen from the pressure storage.

In literature, the compressor is modeled using one of two assumptions for the operational behavior. The compressor is modeled by using the specific work polytropic compression [40], or the specific work for isentropic compression [41]. In this work, the work for isentropic compression [42] is considered as an assumption to approximate the electricity consumption of the compressor p^{comp}

$$p^{\mathrm{comp}} = \frac{n^{\mathrm{H2,comp}}}{\eta^{\mathrm{comp}}} \cdot \frac{\kappa}{\kappa - 1} R T^{\mathrm{in}} \cdot \left[\left(\frac{pr^{\mathrm{comp,out}}}{pr^{\mathrm{comp,in}}} \right)^{\frac{\kappa-1}{\kappa}} - 1 \right] \tag{2}$$

where κ is the heat capacity ratio, $pr^{\mathrm{comp,out}}$ pressure at the outlet, $pr^{\mathrm{comp,in}}$ is the pressure at the inlet, n^{comp} is the hydrogen input, T^{in} is the initial gas temperature, and η^{comp} is the compressor efficiency. A compressor efficiency of $\eta^{\mathrm{comp}} = 82.5\,\%$ is utilized as done by Scheepers et al. [41]. Thus, the electricity consumption of the compressor is approximated by the specific isentropic work for compression and the assumption of a

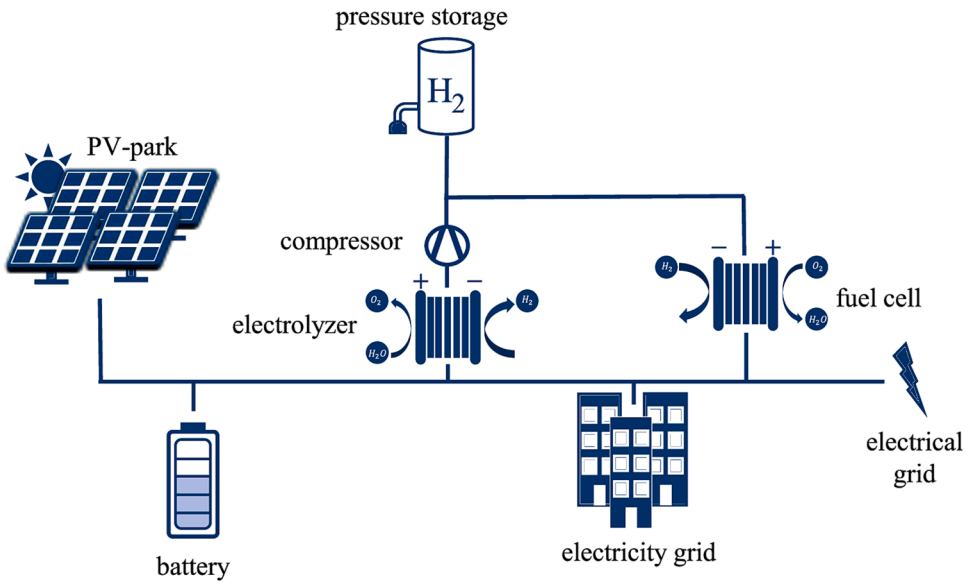

Fig. 1. Sketch of the energy system.

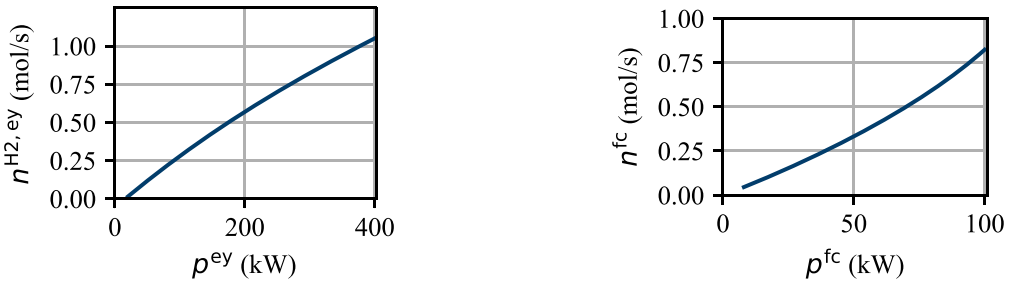

(a) electrolyzer (b) fuel cell

Fig. 2. Visualization of operational behavior of the electrolyzer and the fuel cell. (a) visualizes the hydrogen output of the electrolyzer as a function of the electricity input. (b) visualizes the hydrogen consumption of the fuel cell as a function of the electricity output.

constant compressor efficiency. The hydrogen input into the compressor is equal to the hydrogen output of the electroylzer

$$n^{comp} = n^{H2,ey} \tag{3}$$

The electrical power produced by the PV park and the electricity demand are precalculated and set as parameters in the simulation system to enable perfect foresight for the optimization problem. The electricity demand is derived from the combined electricity consumption of multiple office buildings of the research center in Jülich, with a maximal electrical consumption of 300 kW. The average electricity consumption is 160 kW, while the base load is around 130 kW. The data for the PV park is calculated using the open-source Python package pvlib [43] and the global horizontal irradiation, the global diffuse irradiation, the wind speed, and the air temperature measured by the weather station in Aachen Orsbach from the year 2020 as provided by the dwd [44]. The resulting PV power and the electricity demand considered in this work are shown in Fig. 3.

Table 1 shows an overview of the component sizes based on the component sizes of the hydrogen storage system of the Living Lap Energy Campus project [45].

Table 1
Component sizes of the energy system.

Component Name	Parameter	Value
PV park	$p^{PV,peak}$	1600 (kW)
Electrolyzer	$p^{ey,max,el}$	400 (kW)
Fuel Cell	$p^{fc,max,el}$	100 (kW)
Battery	$p^{bat,max,el}$	100 (kW)
	C^{bat}	600 (kWh)
Pressure Tank	$pr^{ps,max}$	50 (bar)
	V^{ps}	30.238 (m^3)

2.2. Model generation

The simulation models are utilized to generate the MILP optimization models of the fuel cell, the electrolyzer, and the compressor, using the modeling toolbox LinMOG described in [46]. The univariate models of the electrolyzer and the fuel cell are derived using the Python toolbox pwlf [47] while the model of the compressor is derived using an implementation of the hinging hyperplane tree algorithm that is described by Kämper et al. [48]. The procedure for the model generation is described in more detail in [46]. For the sake of readability, the general procedure is shortly explained for the compressor and visualized in Fig. 4.

First, an ideal hydrogen source, sink, and an ideal electrical source are connected to the simulation model of the compressor. Next, the pressure of the hydrogen source is set to 2 bar while the pressure of the sink, and the hydrogen flow, are not fixed. By varying the energy equivalent hydrogen flow rate $w^{comp,H_2,in}$ based on the LHV and the pressure $pr^{comp,out}$ at the outlet of the compressor, the electricity consumption p^{comp} at different operating points of the compressor is simulated. The electricity consumption calculated with this procedure and the operating conditions $w^{comp,H_2,in}$ and $pr^{comp,out}$ are then utilized as input for the modeling toolbox to derive a model of the operational behavior. The piecewise linear model is then parsed to different MILP formulations as described by Vielma et al. [49].

The resulting models of the operational behavior for the fuel cell with five linear elements and the electrolyzer with four linear elements are shown in Fig. 5. The model of the fuel cell relates the hydrogen input w^{fc,H_2} based on the LHV with the electricity output p^{fc}, while the model of the electrolyzer relates the power input of the electrolyzer p^{ey} with the hydrogen output $w^{ey,H2,out}$ based on the LHV. The resulting piecewise linear model of the compressor with four linear elements is shown in Fig. 6. A detailed investigation of the model accuracy, including an analysis of the predictive capabilities of the piecewise linear models, is done in [46]. Five linear elements were chosen for the fuel cell to reduce the average modeling error such that the average modeling error is

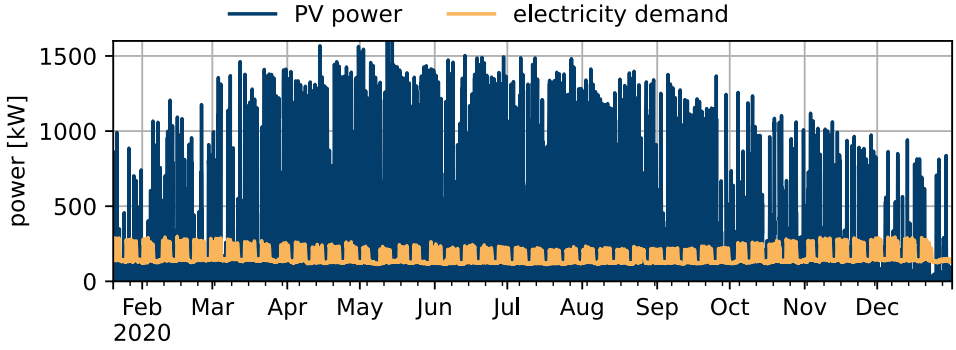

Fig. 3. Visualization of the considered electricity demand and PV power.

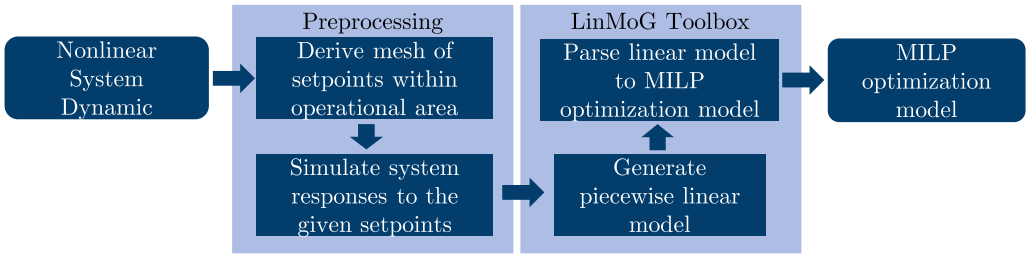

Fig. 4. Visualization of the model generation procedure. Figure based on [46].

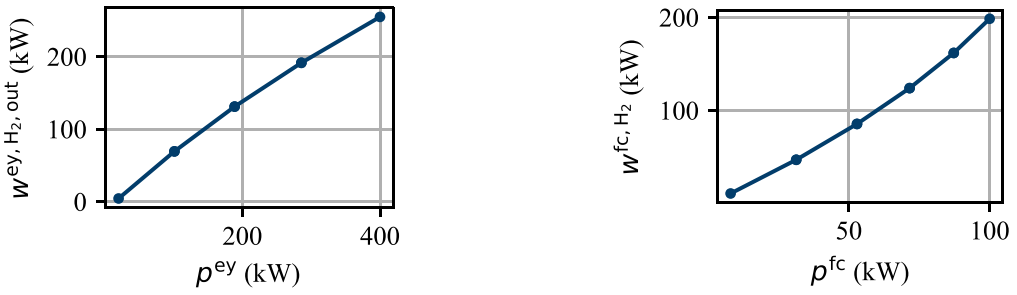

(a) electrolyzer (b) fuel cell

Fig. 5. Visualization of the piecewise linear model of the operational behavior of the electrolyzer and the fuel cell. The electrolyzer model visualized in (a) relates the power input p^{ey} with the hydrogen output $w^{ey,H2,out}$ based on the LHV. The fuel cell model shown in (b) relates the hydrogen input w^{fc,H_2} based on the LHV with the electricity output p^{fc}. The blue dots represent the breakpoints of the piecewise linear functions.

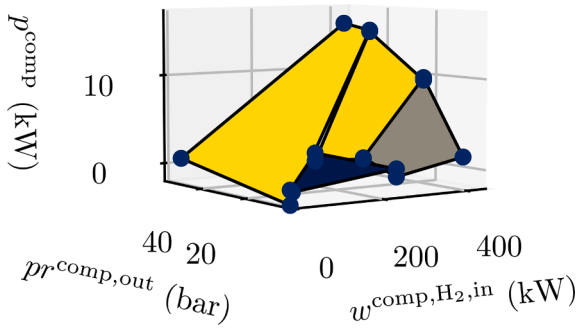

Fig. 6. Visualization of the piecewise linear model of the compressor. $pr^{comp,out}$ is the output pressure of the compressor, $w^{comp,H_2,in}$ is the energy equivalent hydrogen flow rate based on the LHV, and p^{comp} is the electricity consumption of the compressor.

similar between all components at around 0.239 kW or less.

2.3. Optimization model

The optimization model of the whole energy system is derived using the object-oriented open-source framework COMANDO [50]. The electrical power of the PV park at each time step t, p_t^{PV} as well the electricity demand p_t^{ed} are parameters in the optimization problem that are set using the forecasted data for each time step.

The operational behavior of the electrolyzer and the fuel cell are determined by piecewise linear models shown in the previous section. A binary variable b_t^{op} is added to the piecewise linear models to enable a full shutdown of the fuel cell and the electrolyzer. Thus, an additional point at 0 is added to the piecewise linear model.

The change in the state of charge of the pressure storages is modeled using the storage capacity C^{ps}, and the ingoing and outgoing energy flows $w_t^{H_2,in}$ and $w_t^{H_2,out}$

$$\Delta soc_t^{ps} = \frac{(w_t^{ps,H_2,in} - w_t^{ps,H_2,out}) \cdot \Delta t}{C^{ps}}, \tag{4}$$

where Δt is the time step width of time step t. The index t is omitted as the time step width is equal for all time steps in this investigation. The capacity is calculated using the ideal gas law with the storage volume $V^{ps} = 30.238\ m^3$, the storage temperature $T^{ps} = 293.15$ K, the universal gas constant R, the minimal storage pressure $pr^{ps,min} = 5$ bar, maximal storage pressure $pr^{ps,max} = 50$ bar, and the lower heating value of hydrogen LHV = 241.818 kJ/mol

$$C^{ps} = \frac{V^{ps} \cdot LHV}{T^{ps} \cdot R} \cdot \left(pr^{ps,max} - pr^{ps,min}\right) = 3749.95 \text{kWh}. \tag{5}$$

The state of charge in time step t, soc_t^{ps} is calculated using Δsoc_t^{ps}, and the previous state of charge soc_{t-1}^{ps}

$$soc_t^{ps} = soc_{t-1}^{ps} + \Delta soc_t^{ps}. \tag{6}$$

The pressure within the pressure storage tank pr_t^{ps} is calculated using the state of charge and the minimal and maximal storage pressures

$$pr_t^{ps} = soc_t^{ps} \cdot \left(pr^{ps,max} - pr^{ps,min}\right) + pr^{ps,min}. \tag{7}$$

The modeling of the BSS is done similarly. A change in the state of charge is calculated by

$$\Delta soc_t^{bat} = \frac{\left(p_t^{bat,ch} \cdot \eta^{bat,ch} - p_t^{bat,dis} / \eta^{bat,dis}\right) \cdot \Delta t}{C^{bat}}, \tag{8}$$

where $\eta^{bat,ch}$ and $\eta^{bat,dis}$ are the charging and discharging efficiencies.The state of charge in timestep t soc_t^{bat} is then calculated by

$$soc_t^{bat} = soc_{t-1}^{bat} + \Delta soc_t^{bat} \tag{9}$$

Two additional constraints are added to ensure that the battery is only charging or discharging at the same time

$$p_t^{bat,ch} \leqslant b_t^{op,bat} \cdot p^{bat,max,el}, \tag{10}$$

$$p_t^{\mathrm{bat,dis}} \leqslant \left(1 - b_t^{\mathrm{op,bat}}\right) \cdot p^{\mathrm{bat,max,el}}. \tag{11}$$

For the modeling of the compressor, the operational behavior is first derived as described in the previous section. The output pressure of the compressor $pr_t^{\mathrm{out,comp}}$ needs to be equal to the storage pressure pr_t^{ps} if the compressor is operated. Otherwise, the output pressure must be zero in order to utilize the piecewise linear model. This is achieved by introducing a binary variable $b_t^{\mathrm{op,comp}}$ and the following equations

$$pr_t^{\mathrm{comp,out}} \leqslant pr^{\mathrm{ps,max}} \cdot b_t^{\mathrm{op,comp}} \tag{12}$$

$$pr_t^{\mathrm{comp,out}} + pr^{\mathrm{ps,max}} \cdot (1 - b_t^{\mathrm{op,comp}}) \geqslant pr^{\mathrm{ps}} \tag{13}$$

$$pr_t^{\mathrm{comp,out}} \leqslant pr_t^{\mathrm{ps}} \tag{14}$$

The ingoing hydrogen flow $w_t^{\mathrm{comp,H_2,in}}$ is equal to the outgoing hydrogen flow from the electrolyzer, and since it is assumed that no losses occur within the compressor, the outgoing hydrogen flow $w_t^{\mathrm{comp,H_2,out}}$, is also the same as the ingoing hydrogen flow.

$$w_t^{\mathrm{ps,H_2,in}} = w_t^{\mathrm{ey,H_2,out}} = w_t^{\mathrm{comp,H_2,in}} = w_t^{\mathrm{comp,H_2,out}} \tag{15}$$

Similarly, the outgoing hydrogen flows of the pressure storage tank are equal to the ingoing hydrogen flows of the fuel cell:

$$w_t^{\mathrm{ps,H_2,out}} = w_t^{\mathrm{fc,H_2}} \tag{16}$$

Finally, the electrical energy drawn from the grid $p_t^{\mathrm{grid,buy}}$ as well as the electrical energy feed into the grid $p_t^{\mathrm{grid,in}}$ are calculated using the electrical energy from the PV park p_t^{PV}, the electricity demand p_t^{ed}, the charging and discharging power of the battery $p_t^{\mathrm{bat,ch}}, p_t^{\mathrm{bat,dis}}$ as well as the electricity demand of the electrolyzer p_t^{ey}, the electrical energy produced by the fuel cell p_t^{fc} and the electricity demand by the compressor p_t^{comp}

$$0 = p_t^{\mathrm{grid,buy}} - p_t^{\mathrm{grid,in}} + p_t^{\mathrm{PV}} - p_t^{\mathrm{ed}} + p_t^{\mathrm{bat,dis}} - p_t^{\mathrm{bat,ch}} - p_t^{\mathrm{ey}} + p_t^{\mathrm{fc}} - p_t^{\mathrm{comp}}. \tag{17}$$

To ensure that no energy is drawn from the grid and fed into the grid at the same time, a binary variable $b^{\mathrm{op,grid}}$ and the following two equations are added

$$p_t^{\mathrm{grid,buy}} \leqslant b_t^{\mathrm{op,grid}} \cdot w^{\mathrm{grid,max,el}}, \tag{18}$$

$$p_t^{\mathrm{grid,in}} \leqslant (1 - b_t^{\mathrm{op,grid}}) \cdot w^{\mathrm{grid,max,el}}, \tag{19}$$

where $w^{\mathrm{grid,max,el}}$ is the maximal electricity that can be drawn or fed into the grid, this factor is set to $w^{\mathrm{grid,max,el}} = 20000$ kW since no limitations are considered for the grid.

Furthermore, the following equations are added to set the current system state of the simulation model as the starting point of the optimization problem:

$$soc_1^{\mathrm{ps}} = soc_{t^{\mathrm{sim}}}^{\mathrm{ps}} + \Delta soc_1^{\mathrm{ps}}, \tag{20}$$

$$soc_1^{\mathrm{bat}} = soc_{t^{\mathrm{sim}}}^{\mathrm{bat}} + \Delta soc_1^{\mathrm{bat}}, \tag{21}$$

where $soc_{t^{\mathrm{sim}}}^{\mathrm{ps}}$ and $soc_{t^{\mathrm{sim}}}^{\mathrm{bat}}$ are the states of charge of the pressure storage tank and the battery of the simulation in time step t^{sim}. The interaction between the optimization and the simulation is described in more detail in Section 2.4.

As an objective, the electricity drawn from the grid is selected

$$Obj = \sum_{t=1}^{T} p_t^{\mathrm{grid,out}} \cdot \Delta t \tag{22}$$

where T is the last timestep within the prediction horizon. Thus, the electricity drawn from the grid is minimized while the electricity fed into the grid is not considered. This objective is chosen to increase the share of renewable energies utilized to satisfy the electricity demand.

An additional minimal operational and shutdown time for the operation of the fuel cell and the electrolyzer is considered in Section 4.5. A minimal operational and shutdown time within the optimization model is achieved by adding a binary variable for a start-up st^{c} and the shutdown sd^{c} to the model of component c. The constraints

$$st_t^{\mathrm{c}} \geqslant b_t^{\mathrm{op,c}} - b_{t-1}^{\mathrm{op,c}}, \tag{23}$$

$$st_1^{\mathrm{c}} \geqslant b_t^{\mathrm{op,c}} - b_{t^{\mathrm{sim}}}^{\mathrm{op,c}}, \tag{24}$$

$$sd_t^{\mathrm{c}} \geqslant b_{t-1}^{\mathrm{op,c}} - b_t^{\mathrm{op,c}}, \tag{25}$$

$$sd_1^{\mathrm{c}} \geqslant b_{t^{\mathrm{sim}}}^{\mathrm{op,c}} - b_1^{\mathrm{op,c}}, \tag{26}$$

ensure that st_t^{c} in time step t is one if the component is switched on and sd_t^{c} is one if component c is shut off. In Eqs. 24 and 26 $b_{t^{\mathrm{sim}}}^{\mathrm{op,c}}$ is the current operational state of the component in timestep t^{sim} of the simulation. Since no start-up or shutdown costs are considered, sd_t^{c} and st_t^{c} do not need to be set to 0 if no state change occurs.

The minimal operational and shutdown $t^{\mathrm{sd,op}}$ time is then enforced by the constraints

$$n^{\mathrm{op}} = n^{\mathrm{sd}} = t^{\mathrm{sd,op}} / \Delta t \tag{27}$$

$$st_t^{\mathrm{c}} \cdot n^{\mathrm{op}} \leqslant \sum_{i=t}^{t+n^{\mathrm{op}}} b_i^{\mathrm{op,c}} \tag{28}$$

$$(1 - sd_t^{\mathrm{c}}) \cdot n^{\mathrm{sd}} \geqslant \sum_{i=t}^{t+n^{\mathrm{sd}}} b_i^{\mathrm{op,c}} \tag{29}$$

where $n^{op,st}$ is the number of time steps in the operational state or shutoff state. Thus, the optimization ensures that the system state can only be changed if the minimal time $t^{\mathrm{sd,op}}$ has passed.

2.4. Model predictive control framework

In the following, the framework utilized to couple the optimization model described in Section 2.3 with the simulation model described in Section 2.1 is explained. The simulation model is written in Modelica and translated into a functional mock-up unit (FMU). Using the Python package FMPy [51] the system behavior of the hybrid energy system can be simulated within a Python environment. Therefore, the whole framework can be run in a Python environment. Fig. 7 shows a visualization of the MPC-framework.

The MPC framework keeps track of the current time step t^{sim} and derives time stamps for each data point of the optimization results according to the current time and the time step width. Thus, the optimization results can be stored temporarily as time-stamped data. For any point within the prediction horizon t^{pred}, the operational strategy, as calculated by the optimization, can be retrieved. This enables the simulation to run completely independent of the optimization in a much finer temporal resolution. Furthermore, storing the optimization results as time-stamped data allows an easy adaptation of the prediction horizon t^{pred} and the control horizon t^{cont}. The weather and demand data is also time-stamped data. Thus, data can be supplied to the simulation for each point in time, and a perfect forecast according to the prediction horizon can be supplied for the optimization. The simulation results are also stored as time-stamped data such that the MPC framework can supply the current system states $soc_{t^{\mathrm{sim}}}^{\mathrm{bat}}$, $soc_{t^{\mathrm{sim}}}^{\mathrm{ps}}$, $b_{t^{\mathrm{sim}}}^{\mathrm{op,fc}}$, and $b_{t^{\mathrm{sim}}}^{\mathrm{op,ey}}$ to the optimization for each next step of the receding horizon optimization. Fig. 8 shows a sketch of the concept.

3. Case study

The electricity consumption of an energy system controlled by the MPC framework is compared to the electricity consumption of an energy

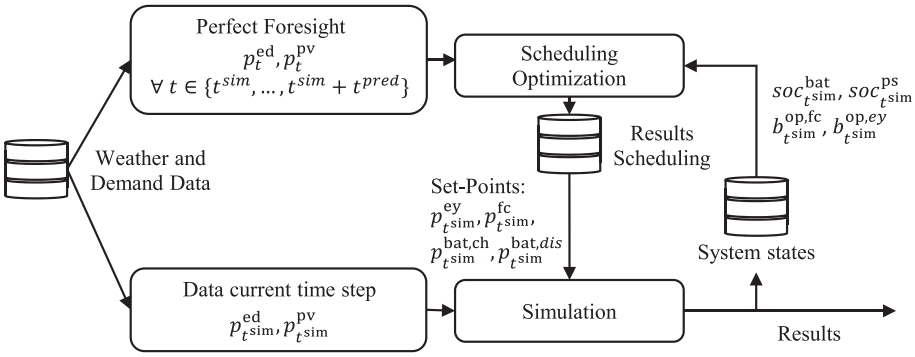

Fig. 7. Visualization of the MPC-framework.

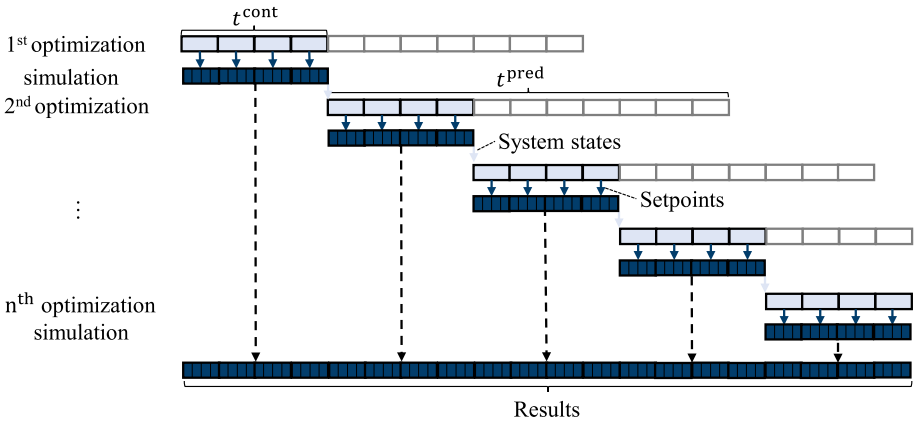

Fig. 8. Visualization of the concept of the MPC-framework.

system controlled by a rule-based controller to evaluate the benefits of MPC. The rule-based controller is described in Section 3.1. Furthermore, clustering is used to decrease the number of optimizations carried out for the case study while still considering the operation of the hybrid energy system throughout the year. The clustering of the year into typical weeks is described in subSection 3.2.

For the derivation of the impact of different parameters on the results of the MPC framework, an investigation on the impact of a varying prediction horizon length, a varying control horizon length, a varying electricity demand, a varying PV power, and the consideration of a variable grid price for multi-objective optimizations is conducted.

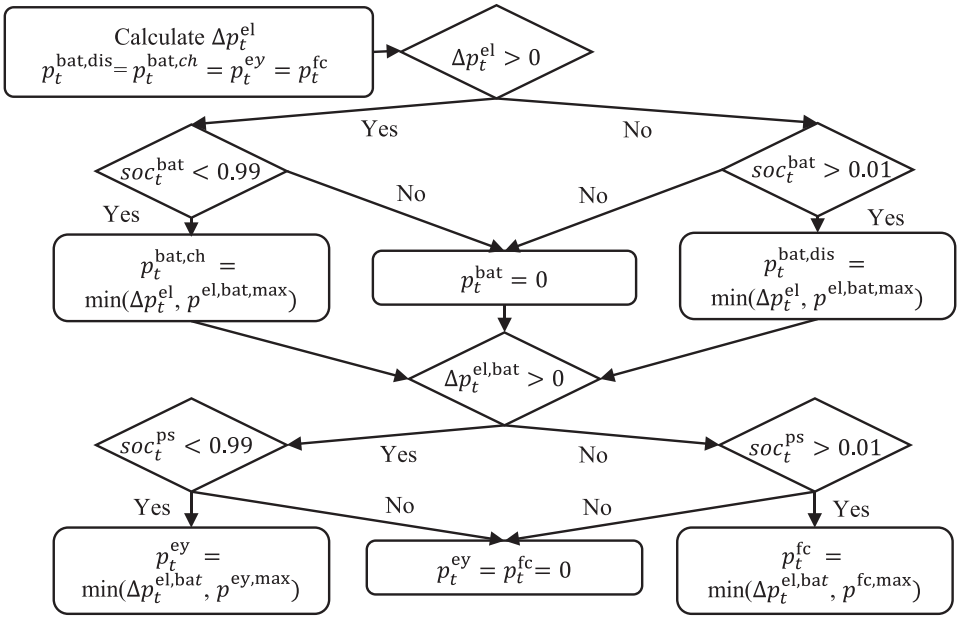

Fig. 9. Flow chart of the rule-based controller considered in this work.

3.1. Rule-based controller

The rule-based controller operates on a set of rules to minimize the energy consumption of the hybrid energy system. If the energy from the PV park p_t^{PV} is larger than the electricity demand p_t^{ed},

$$\Delta p_t^{\mathrm{el}} = p_t^{\mathrm{pv}} - p_t^{\mathrm{ed}} \geqslant 0 \tag{30}$$

the battery starts charging. If the surplus energy is larger than the energy that the battery can utilize,

$$\Delta p_t^{\mathrm{el,bat}} = \Delta p_t^{\mathrm{el}} - p_t^{\mathrm{bat,ch}} + p_t^{\mathrm{bat,dis}} \geqslant 0 \tag{31}$$

for instance, if the battery is full, the electrolyzer starts operating. If p^{PV} is smaller than p^{ed} the battery starts unloading. If more energy is needed than the battery can supply, the fuel cell is turned on to provide the rest of the energy needed. Thus, the battery is always utilized first since its efficiency is higher than the different efficiencies of the hydrogen components. A flowchart of the general principle of the rule-based controller is shown in Fig. 9.

The minimal operational time is enforced by a rule such that the electrolyzer and fuel cell can not change their state for the defined period of time after a previous state change. Therefore, one additional variable is introduced that keeps track of the time of the last state change. In this work, a minimal operational time of 2 h is assumed, similar to the work of Fan et al. [52].

3.2. Clustering

The MPC and the rule-based controller are compared for five typical weeks of the year 2020. The typical weeks and the number of times the week appears within one year are derived with the open-source clustering toolbox tsam [53]. Similar to the work of Kotzur [54], k-medoids clustering is used to derive the typical periods. The electricity price added in Section 4.6 is weighted with a factor of 0 in the clustering to increase the accuracy of the typical periods for the investigations carried out in Sections 4.1–4.5. Then, for the investigation done in Section 4.6, the same typical periods are utilized to achieve comparability between the results.

The electricity consumption over one year is calculated by multiplying the electricity consumption of one typical period by its number of appearances throughout the year. Fig. 10 visualizes the separation of the year into 5 clusters of one week each.

4. Results

This section compares the results of the case study. Therefore, the influence of different settings on the resulting operational strategies is investigated. A comparison between different prediction horizon lengths on the optimization results is made in subSection 4.1. SubSection 4.2 compares optimized and rule-based operations. In 4.3, a sensitivity analysis with regard to the electricity demand and installed photovoltaic capacity is shown. The impact of an increased battery charging and discharging rate is discussed in Section 4.4. Furthermore, Section 4.5 discusses the impact of a minimal operational time for the hydrogen components. Finally, in Section 4.6, the impact of a varying grid price in combination with multi-objective optimizations is discussed utilizing Pareto fronts. All optimizations are carried out using Gurobi [55] with a relative mixed integer programming (MIP) gap of 0.1% and an absolute MIP gap of 0.5 of the objective value on an Intel i5-8265U CPU with 23 GB of RAM.

4.1. Influence of the prediction horizon length

The following subsection investigates the influence of the prediction horizon of the optimization problem. An optimization problem's prediction horizon is an essential parameter since a long-term operational strategy can only be derived if the horizon is chosen sufficiently long. However, a long prediction horizon leads to many time steps and, therefore, an increased optimization problem size. This section chooses a control horizon of 24 h for a quick run time of the MPC framework. The impact of a shorter control horizon is shown in Section 4.6.

First, the operational behavior of the energy system with respect to the prediction horizon of the optimization problem is evaluated. The results of the first optimization of the second typical period are shown in Fig. 11 (a) and (b) for a two-day, a four-day, and a seven-day prediction horizon. As shown, for increasing prediction horizons, different operational strategies are derived from the optimization problem. However, since an optimization problem is solved every 24 h, only the first day of the prediction horizon is used to derive setpoints for the simulation system.

Fig. 12 shows the simulation results of the state of charge of the battery and the pressure storage tank for the whole second typical period. As expected, the simulation results of the first day are almost identical to the optimization results shown in Fig. 11, as the control horizon is set to one day. Thus, the results from the first optimization are utilized to control the energy system during the first day by sending setpoints to the fuel cell, electrolyzer, and battery, as explained in Section 2.4. The simulations of the subsequent days show that different operational points are derived by the optimization in the next step of the receding horizon.

Table 2 shows a comparison between the total grid electricity consumption and the run time of each simulation with model predictive control. As shown in Table 2, increasing the prediction horizon from two to four days leads to a decreased electricity consumption, while increasing the prediction horizon to seven days only leads to slightly better results. Therefore, it can be concluded that many close optimal operating strategies exist, and a four-day prediction horizon is sufficient for this specific system to find close optimal operational points. Utilizing a two-day prediction horizon yields only slightly worse results and thus might be preferable if the run time is limited. However, to utilize the potential of the MPC framework, a four-day horizon prediction horizon is considered in the following investigations.

4.2. Comparison with a rule-based controller

The following section compares exemplary simulation results of the energy system for the third typical period controlled by the MPC framework with the results of an energy system that is controlled by the

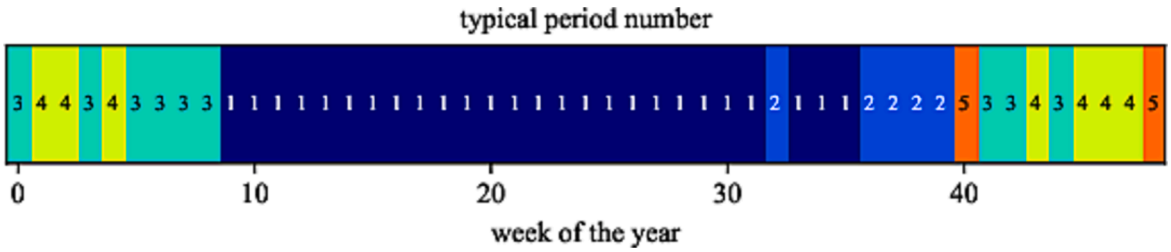

Fig. 10. Clustering results of the year in typical weeks. Each number shows the typical period representing this week in the original data.

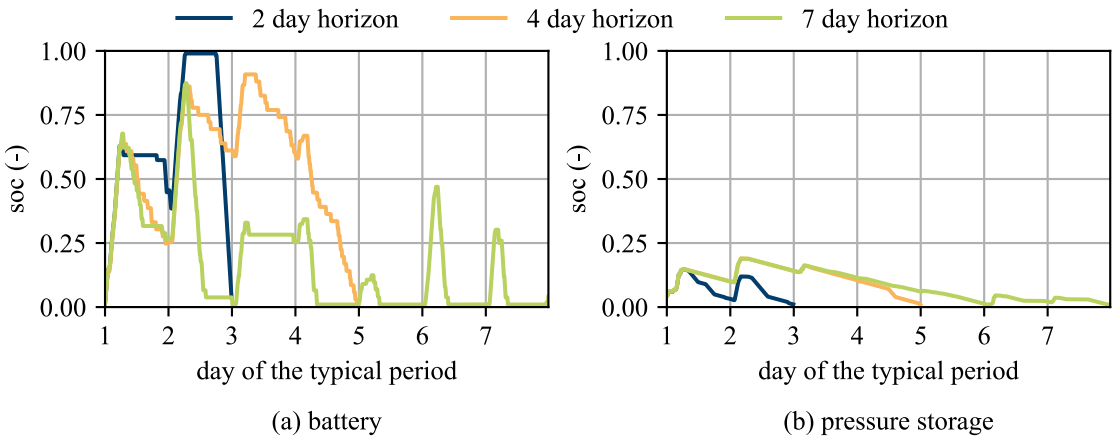

Fig. 11. Comparison between optimization results utilizing a 2-day, 4-day, and 7-day prediction horizon. (a) visualizes the calculated state of charge of the battery, and (b) visualizes the calculated state of charge of the pressure storage.

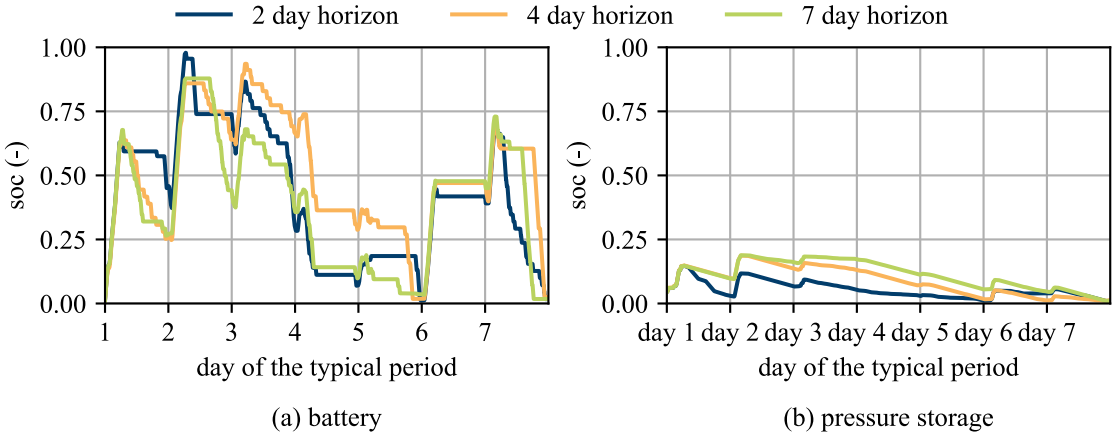

Fig. 12. Comparison between simulation results of the energy system controlled by the MPC framework utilizing a 2-day, 4-day, and 7-day prediction horizon. (a) visualizes the simulated state of charge of the battery, and (b) visualizes the simulated state of charge of the pressure storage.

Table 2
Comparison between the simulated energy drawn from the grid and the runtime by utilizing the MPC framework with 2-day, 4-day, and 7-day prediction horizons.

N_{days}	2-Days	4-Days	7-Days
Electricity Consumption (MWh)	393.92	392.88	392.57
MPC framework run time (min)	6	17	24

rule-based controller. Fig. 13 (a) and (b) show the different operational strategies for the electrolyzer and the fell cell, respectively. The electrolyzer operation is very similar since an excess of energy is available during the day. Therefore, the operating point is determined mainly by the battery's maximal charging capacity and the electrolyzer's nominal power. In comparison, the two operational strategies for the fuel cell are very different. While the rule-based approach utilizes the fuel cell at the beginning of the night in full load, an operation in part load can be observed for the optimized operation.

A comparison between the resulting state of charge (soc) of the battery storage and the hydrogen storage system is shown in Fig. 14 (a) and (b), respectively. One notable difference between both storage technologies is that the discharging is stretched over a more extended period of time for the optimized operation. This shows the model predictive controller's capability to consider future energy production and demand. As a result, less energy is drawn from the electricity grid, as shown in Fig. 15.

Fig. 16, and 17 show the results for the first typical period. A different operational strategy needs to be derived to reduce the utilized grid energy. The energy stored in the battery and the hydrogen storage are utilized in combination to save some battery capacity until the end of the night. The fuel cell setpoint needs to be precisely adapted for this operational strategy. Therefore, a forecast of electricity demand and solar energy is needed. Table 3 shows the grid electricity consumption for each typical period. As shown, during the first typical period, which represents most of the summer, the MPC is able to reduce the electricity consumption by 1.232 MWh. The lowest decrease in the grid consumption is achieved during the second typical period with only 0.15 MWh. This is due to a low utilization of the hydrogen storage system. During the second typical period, only 1.62 MWh of electrical energy is converted to hydrogen, while during the fourth typical period, 3.50 kWh are converted to hydrogen even though less PV energy is available. This difference in the usage of the hydrogen storage system is due to the specific weather and demand conditions of the second and fourth typical periods. The PV power in comparison to the electricity demand is shown in Fig. 18. In the fourth typical period, much excess energy is available during the fourth and fifth days that can be converted to hydrogen for later usage, while the excess energy in the second typical period is mainly stored in the battery.

The total electricity consumption over a whole year is calculated by using the number of times one typical period appears in one year. In this case study, the rule-based approach leads to an electricity consumption of 436.11 MWh, while the optimized operation leads to 392.88 MWh of

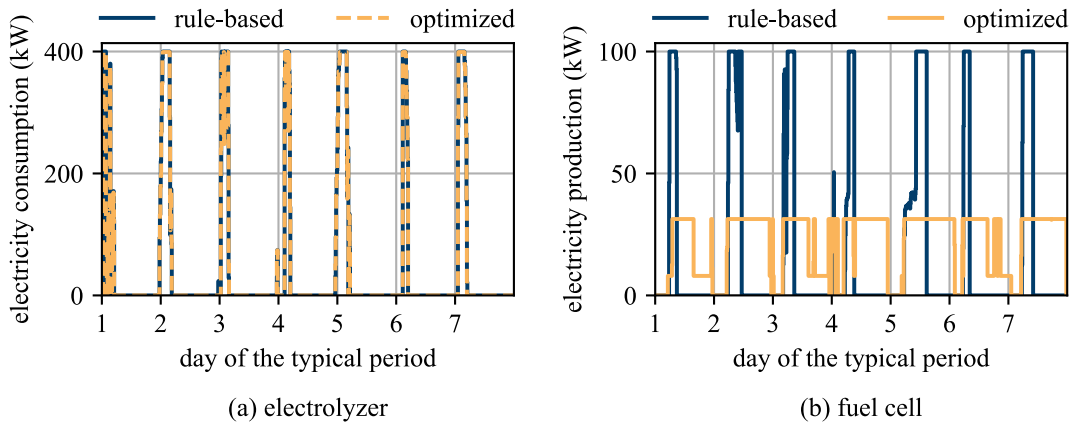

Fig. 13. Comparison between the operational behavior of the electrolyzer and the fuel cell utilizing the MPC framework and the rule-based controller. (a) visualizes the results for the electrolyzer, and (b) visualizes the operation of the fuel cell.

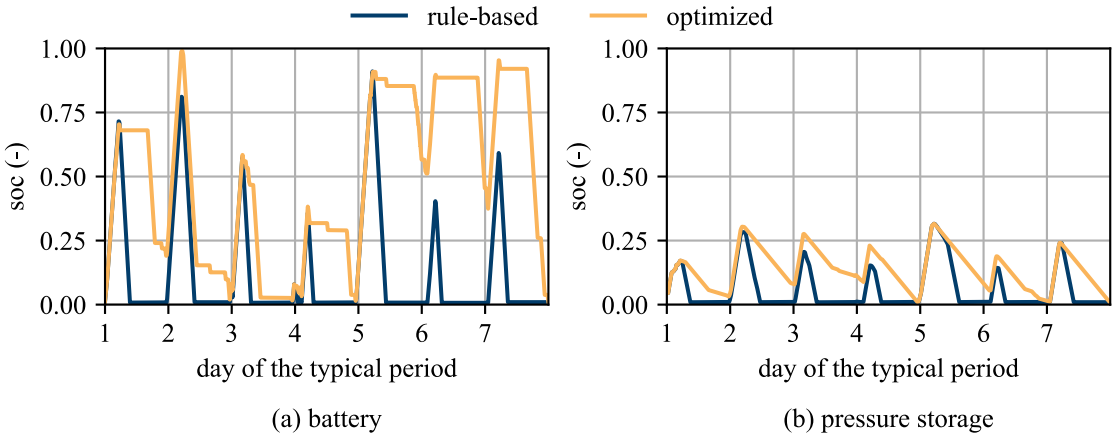

Fig. 14. Comparison between the operational behavior of the storage technologies of the energy system utilizing the MPC framework and the rule-based controller. (a) visualizes the soc of the battery, and (b) visualizes the soc of the pressure storage.

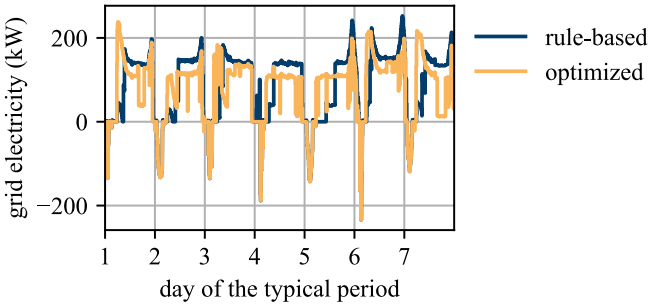

Fig. 15. Comparison between energy drawn from the grid utilizing the MPC framework and the rule-based controller.

energy bought from the grid. Thus, a total reduction of 11% of the total utilized grid energy was achieved using model predictive control.

4.3. Sensitivity analysis

In this section, a sensitivity study is carried out to validate whether model predictive control consistently leads to energy savings compared to a rule-based approach. Therefore, the approach is selected to increase and decrease the energy demand and the available solar energy. In this work, the available solar energy and the energy demand are modified to be at 80% or 120% of the base scenario and run model predictive control and rule-based approach for all resulting scenarios and for the same typical periods as derived in Section 3.2. Similar to Section 4.2, the resulting electricity consumption for the whole year is calculated. Furthermore, the relative difference Δe^{year} between the optimized operation and the rule-based approach is calculated by:

$$\Delta e^{\text{year}} = \frac{E^{\text{RBC}} - E^{\text{MPC}}}{E^{\text{MPC}}} \tag{32}$$

where E^{RBC} and E^{MPC} are the total grid electricity consumptions of the energy system over one year controlled by the MPC and the RBC. The results are shown in Table 4. Some scenarios show a lower relative difference between the optimized operational behavior and the rule-based approach, but at least an improvement of over 3.93% is achieved even in the worst case. This shows that the model predictive controller can increase the system efficiency even in scenarios with scarce and excessive amounts of PV power compared to the electricity demand.

A detailed comparison between the reduction in electricity drawn from the grid ΔE^{cont}:

$$\Delta E^{\text{cont}} = \sum_{i=1}^{N^{\text{tp}}} p_i^{\text{grid,out,RBC,tp}} \cdot \Delta t - \sum_{i=1}^{N^{\text{tp}}} p_i^{\text{grid,out,MPC,tp}} \cdot \Delta t \tag{33}$$

is shown in Table 5. In Eq. 33 $p_i^{\text{grid,out,RBC,tp}}$ is the electricity drawn from the grid by the energy system controlled by the RBC, and $p_i^{\text{grid,out,MPC,tp}}$ is the electricity drawn from the grid by the energy system controlled by the MPC during the i-th typical period tp. Furthermore, N^{tp} is the number

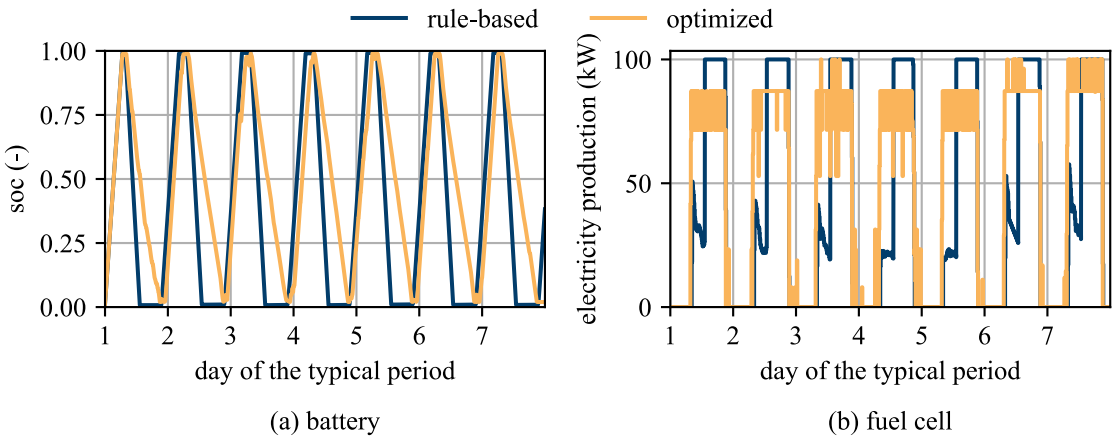

Fig. 16. Comparison between the operational behavior of the battery and the fuel cell utilizing the MPC framework and the rule-based controller. (a) visualizes the soc of the battery, and (b) visualizes the operation of the fuel cell.

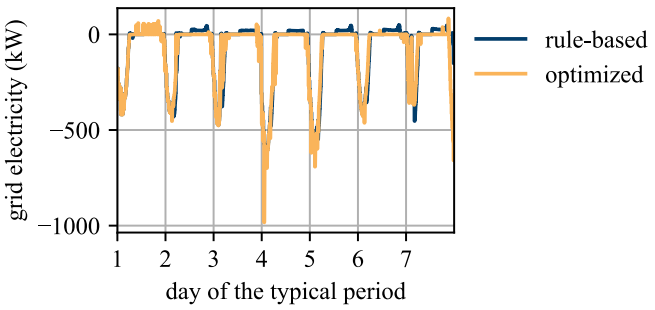

Fig. 17. Comparison between energy consumption of the energy system utilizing the MPC framework and the rule-based controller.

of time steps within the typical period, and Δt is the simulation time step width of 1 min.

As shown in Table 5, the MPC is able to always decrease the electricity drawn from the grid. The most significant differences between runs with different sensitivity factors are notable in the first typical period. The RBC is able to derive good strategies during the first typical period if the electricity demand is low, as it becomes less critical to utilize the energy storage system efficiently. On the contrary, in the third typical period, the difference between the MPC and the RBC does not directly correlate with the electricity demand factor but with the PV factor. This is most likely due to a higher utilization of the storage systems. As shown in Figs. 13–15 during the third typical period, both storage technologies are utilized during the third typical period. However, neither storage is fully charged as not enough renewable energy is

Table 3
Electricity demand, PV energy, and grid electricity consumptions of the energy system controlled by the MPC framework and the RBC for the different typical periods as derived in Section 3.2.

Typical period	1	2	3	4	5
Electricit Demand (MWh)	25.28	27.09	29.63	29.73	25.82
PV Energy (MWh)	56.22	12.87	21.42	10.77	17.35
Electricity Consumption RBC (MWh)	1.41	15.84	15.49	21.98	13.54
Electricity Consumption MPC (MWh)	0.178	15.69	14.69	21.63	13.12

Table 4
Results of the sensitivity analysis.

sensitivity factors		grid electricity		
PV factor	demand factor	rule-based (MWh)	optimization (MWh)	rel. difference (%)
0.8	0.8	316.77	301.88	4.93
0.8	1	471.08	441.15	6.78
0,8	1.2	663.53	638.40	3.93
1	0.8	289.00	272.89	5.90
1	1	436.11	392.88	11.00
1	1.2	601.43	575.50	4.51
1.2	0.8	268.65	251.11	6.98
1.2	1	411.62	367.08	12.14
1.2	1.2	566.36	535.50	5.76

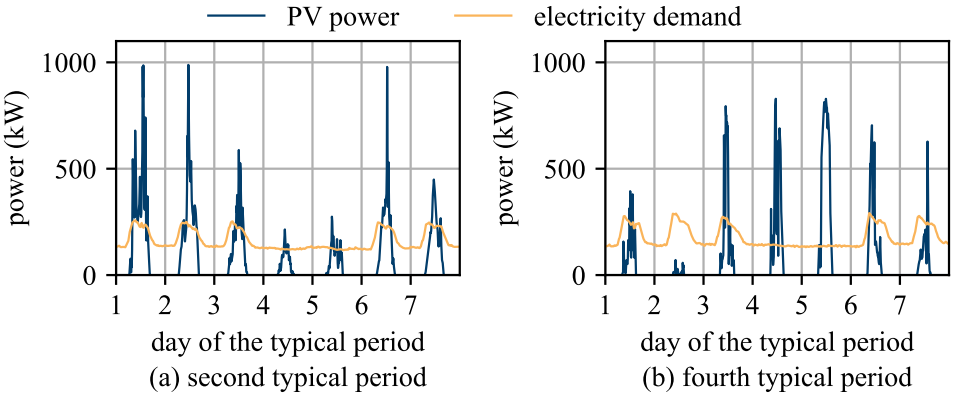

Fig. 18. Visualization of the electricity demand and the PV power during the second and fourth typical period.

Table 5
Reduction of the electricity drawn from the grid ΔE^{cont} in each typical period of the sensitivity analysis.

sensitivity factors		ΔE^{cont} (kWh)				
PV factor	demand factor	tp = 1	tp = 2	tp = 3	tp = 4	tp = 5
0.8	0.8	193.52	119.46	665.58	356.31	386.46
0.8	1	810.35	90.24	634.85	282.91	354.15
0.8	1.2	671.82	92.73	539.65	242.94	319.23
1	0.8	162.61	209.62	776.76	413.90	472.31
1	1	1229.72	146.19	798.25	356.91	419.46
1	1.2	581.59	166.33	761.31	325.22	425.15
1.2	0.8	155.16	304.33	842.73	464.40	569.37
1.2	1	1230.04	219.59	864.56	392.68	466.09
1.2	1.2	704.51	226.73	859.55	385.99	485.02

available. Furthermore, the results show that the improvements to be gained from the model predictive controller depend on the specific typical period.

4.4. Increased battery charging rate

The charging and discharging rate of the battery storage system was chosen low at 100 kW to reduce stress on the battery from fast charging. However, to investigate the effect of a higher charging and discharging rate, the sensitivity analysis is run with $p^{bat,max,el} = 600$ kW. The results are shown in Table 6.

As shown by increasing the charging and discharging rate, the energy systems controlled by the MPC need considerably less grid energy to fulfill the electricity demand. The performance of the rule-based controller even worsens in some cases. This can be explained by faster discharging of the battery such that the fuel cell operates more hours at full load, decreasing the system efficiency.

In summary, the optimization performs even better with an increased charging and discharging rate compared to a rule-based controller. However, an increased charging and discharging rate can also lead to faster battery degradation. Therefore, the charging rate of $p^{bat,max,el} =$ 100 kW is utilized for the following investigations.

4.5. Minimal operational time

A typical constraint to avoid rapid start-ups and shutdowns of the hydrogen components under real-world conditions is incorporating time coupling constraints. This case study assumes a minimal operational and shutdown time of 2 h, similar to Fan et al. [52].

Using a minimal operational time of 2 h leads to a steep decrease in the number of start-ups and shutdowns of the hydrogen components. The number of start-ups and shutdowns of the electrolyzer over one year decreased by 42.09 % from 506 to 293 by utilizing a minimal operational time. The number of start-ups and shutdowns of the fuel cell decreased by 24 % to 879 start-ups and shutdowns, showing that the approach of a minimal operational and shutdown time works to reduce the number of state changes.

The same sensitivity analysis is conducted as in the previous section to investigate the impact of a minimal operational time on the electricity drawn from the grid. The results are shown in Table 7. The electricity consumption increases for both controllers. However, it is noticeable that the relative difference between the rule-based controller and the model predictive controller increases across all cases. Thus, it can be concluded that MPC can handle additional constraints, such as a minimal operational time, more effectively than the rule-based controller.

4.6. Pareto analysis

Under real circumstances, optimizing the electricity price while reducing the electricity consumption might be preferable if electricity is bought at a variable grid price. Therefore, multiobjective optimization can be used to find Pareto-optimal solutions for scheduling the hybrid battery-hydrogen energy system. Thus, a factor ϵ and an additional term for a variable grid price are utilized in the objective function

$$Obj_{new} = \sum_{t=1}^{T} p_t^{grid,buy} \cdot \left(\epsilon + (1-\epsilon) \cdot c_t^{grid}\right) \cdot \Delta t_t \tag{34}$$

where c_t^{grid} is a variable grid price. Thus, if $\epsilon = 1$, an optimization of the consumed grid electricity is carried out, and $\epsilon = 0$ results in a fully economic optimization. The assumption is selected to exclude the option of selling electricity to the grid from the objective function, to reduce the number of influencing factors as much as possible, and to concentrate purely on the operation of the hybrid energy storage system. The electricity price for the year 2020 from the German electricity market is selected as the cost factor c_t^{grid}.

The following investigates the impact of different settings of the MPC framework to analyze the impacts on the Pareto optimal results and, therefore, the theoretical potentials of mathematical optimization for the determination of operational strategies for this particular hybrid energy system. Fig. 19 shows the impact of the prediction horizon on the Pareto optimal solutions.

The resulting Pareto fronts show that optimizations with a prediction horizon of 7 days yield the best results. However, the Pareto fronts of runs of the MPC framework with 2-day and especially 4-day horizons yield only slightly worse results. On the contrary, a run of the MPC framework with a one-day prediction horizon yields much worse results but still performs better than the rule-based controller in most cases. The poor performance of the MPC framework with a 1-day prediction horizon is in part due to the one-day control horizon. However, even with these suboptimal settings for the MPC framework, a decrease in both cost and electricity consumption was achieved with the correct settings, showing the potential capabilities of the approach. All runs considering the rule-based controller result in the same operational strategy since it follows the same rules stated in Section 3.1 for each run of the

Table 6
Results of the sensitivity analysis with an increased charging and discharging rate of the battery.

sensitivity factors		grid electricity		
PV factor	demand factor	rule-based (MWh)	optimization (MWh)	rel. difference (%)
0.8	0.8	303.72	288.93	5.12
0.8	1	484.16	422.39	14.63
0.8	1.2	681.11	619.70	9.91
1	0.8	276.34	251.66	9.81
1	1	431.38	372.45	15.82
1	1.2	618.71	555.75	11.33
1.2	0.8	255.72	227.37	12.47
1.2	1	403.22	342.06	17.88
1.2	1.2	572.97	510.83	12.17

Table 7
Results of the sensitivity analysis with a minimal operational and shutdown time of two hours for the electrolyzer and the fuel cell.

sensitivity factors		grid electricity		
PV factor	demand factor	rule-based (MWh)	optimization (MWh)	rel. difference (%)
0.8	0.8	323.36	303.56	6.52
0.8	1	474.89	443.28	7.13
0,8	1.2	666.60	640.80	4.02
1	0.8	295.99	274.18	7.95
1	1	440.18	395.12	11.41
1	1.2	605.62	577.59	4.85
1.2	0.8	271.73	252.97	7.42
1.2	1	415.94	369.73	12.50
1.2	1.2	569.79	537.80	5.95

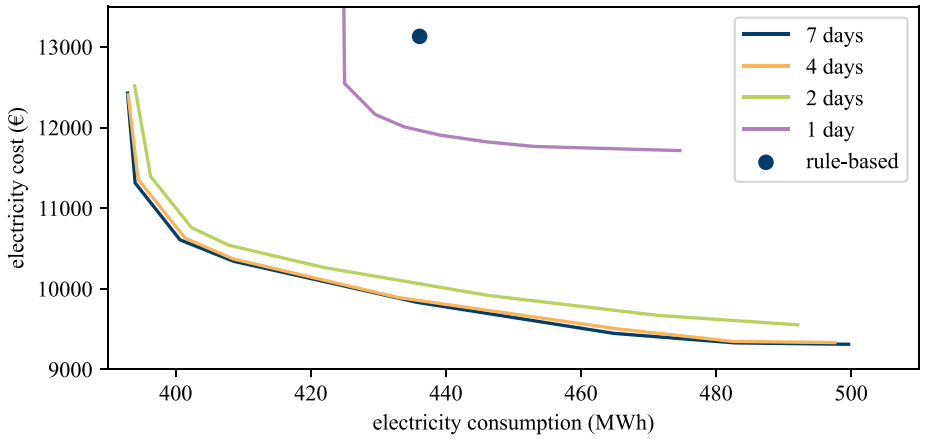

Fig. 19. Visualization of the Pareto front for runs of the MPC framework with different prediction horizons and a control horizon of 24 h.

framework.

To investigate the impact of the control horizon, a reduction of the control horizon for different prediction horizon lengths is investigated. This investigation is done for a prediction horizon of one day, two days, and four days, with a control horizon of 24 h, 12 h, and 6 h. Furthermore, in the case of a one-day prediction horizon, a run of the MPC framework with a control horizon of 1 h is included. The resulting Pareto fronts are shown in Fig. 20 (a)-(c). (a) visualizes the results for a prediction horizon of 1 day, (b) and (c) the results with a two-day and four-day prediction horizon, respectively.

As shown in (a), when a very short prediction horizon is considered, frequent updates of the operational strategies are needed in order to utilize MPC efficiently. In the case of a two-day and a four-day prediction horizon, the benefit of more frequent optimization reduces with longer prediction horizons, as accurate models of the simulation systems are derived in the scope of this work, and perfect foresight is utilized to investigate the potential of MPC. However, under real circumstances, frequent optimization of the operational strategy will most likely increase the performance of MPC due to uncertainties in the optimization model and the forecasted data.

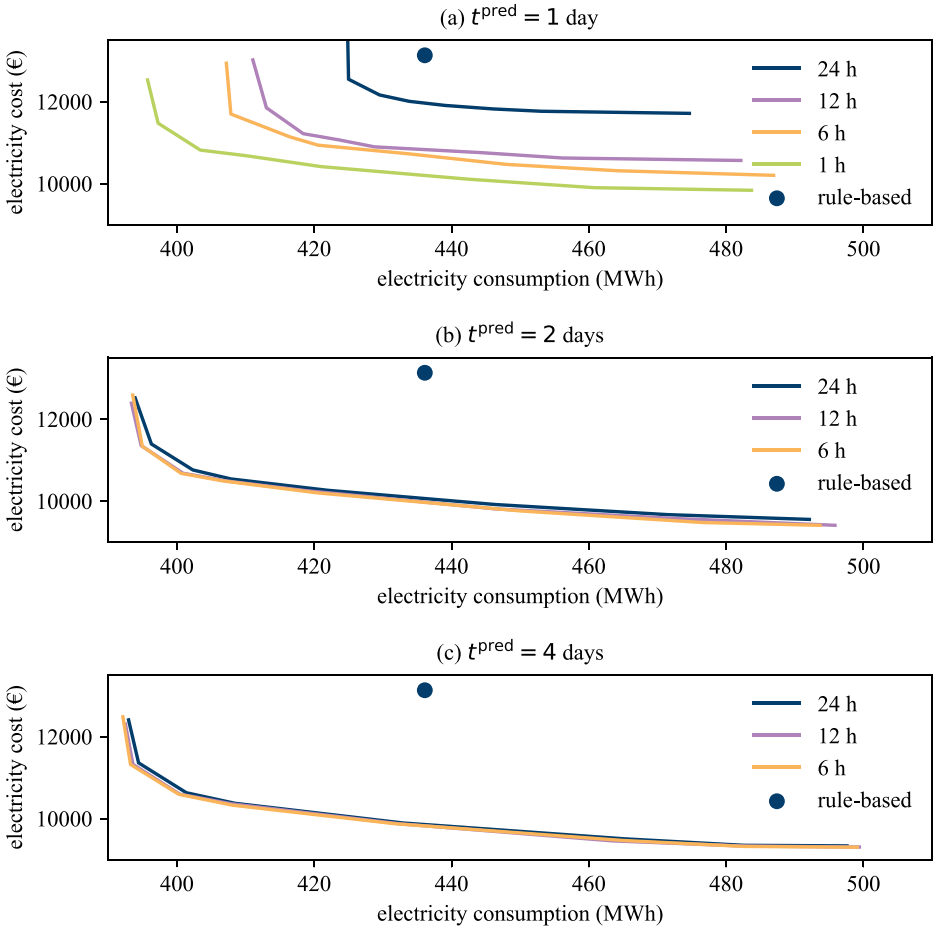

Fig. 20. Visualization of the Pareto front for runs of the MPC framework with different prediction horizons and different control horizons. (a) shows the results for a prediction horizon of 1 day, (b) shows the results for a prediction horizon of 2 days, and (c) shows the results for a prediction horizon of 4 days.

Furthermore, the influence of the price forecast horizon on the results of the MPC framework is investigated. Since a price forecast of multiple days is, in most cases, not available, the prediction horizon of the price is reduced to 24 h. Moreover, the control horizon is set to 12 h, so the operational strategy can be adapted twice daily. For the prediction horizon beyond the first 24 h, a constant price of 30.93 €/MWh is considered. The MPC framework is run using a prediction horizon of 4 days and a prediction horizon of 2 days. Runs with the two-day prediction horizon are referred to as case one, and the runs with the four-day horizon are referred to as case 2. The resulting Pareto fronts are shown in Fig. 21 in comparison to the runs of the MPC framework with a one-day prediction horizon and a seven-day prediction horizon with full perfect foresight, and a one-day control horizon as shown in Fig. 19.

Both cases show a small dependency on the parameter ∈. This is because a constant price is assumed for a large part of the prediction horizon. A constant electricity price turns the optimization of the electricity cost into an optimization of the consumed grid electricity. Thus, the optimization prioritizes energy efficiency over cost efficiency. As expected, an increased prediction horizon leads to increased efficiency. However, this effect is relatively small, showing that a one-day prediction horizon is insufficient to reduce the operational cost to the full extent possible. However, a two-day prediction horizon of the energy availability can lead to drastic decreases in energy consumption while drastically reducing the operational cost compared to a rule-based controller.

A fully variable grid price might not be desired in some practical applications. Therefore, a variable grid price with time-specific static electricity prices might be preferred under some circumstances. Therefore, an investigation is carried out using a three-tier time-of-use concept as explained by Stute et al. [56] to investigate potential improvements to be gained by the developed MPC approach with fixed time-dependent electricity prices. In this study, the same three time periods are applied as utilized by Stute et al. [56]. In this work, the electricity price during each period is the yearly average during that time period. Thus, a constant electricity price of $c^{\mathrm{grid},1} = 31.54$ €/MWh is considered for the time between 6 a.m. and 4 p.m. Furthermore, during the time between 4 p.m. and 9 p.m., a constant price of $c^{\mathrm{grid},2} = 37.74$ €/MWh is considered, while a price of $c^{\mathrm{grid},3} = 26.29$ €/MWh is considered for the time between 9 p.m. and 6 a.m. As shown in Fig. 22, the model predictive controller is able to reduce the electricity cost considering a three-tier time-of-use concept. However, when considering a three-tier time-of-use concept, the potential reduction in the operating cost is limited. This is due to the low electricity price at night when no PV energy is available, and energy is drawn from the grid. The best results are achieved with a 7-day prediction horizon. However, increasing the prediction horizon above two days yields only slightly better results. This is similar to the results with a fully variable grid price. However, a fully variable grid price with a seven-day prediction horizon leads to a 20% cost reduction. In comparison to the more realistic scenario with an accurate price prediction of one day, the tree-tier-time of use concept achieved similar results with a reduction in the operational cost below 1%. This shows that in the case study investigated in this paper, a three-tier time-of-use concept leads to comparable results to a fully variable grid price if the price forecast is limited to one day. However, this case study also shows that MPC can potentially decrease the operational cost drastically if accurate long-term forecasts on the electricity price can be obtained.

5. Conclusion

This work utilizes a simulation model of a hybrid energy storage system to derive tailor-made MILP optimization models of the operational behavior using the open-source toolbox LinMOG. The derived MILP optimization models of the operational behavior are combined with additional constraints to derive component models in the COMANDO framework [50]. The component models are then combined into a MILP optimization model of the hybrid energy system. The optimization model is used to determine operating strategies for the hybrid energy storage system in the context of a model predictive control framework. In order to compare different MPC-based operational strategies, a framework is developed that enables a quick way to test many different settings for a model predictive controller. In future works, the operational behavior of the simulation model could be validated using a hadware-in-the-loop platform such as explained in [57].

The model predictive controller is compared to a rule-based controller to show the potential improvements to be gained by utilizing model predictive control under various external conditions. Therefore, a sensitivity analysis is conducted by varying the PV power and the electricity demand. For this study, five typical weeks are derived with k-medoids clustering to investigate the average yearly electricity consumption emerging from utilizing either controller. It was shown that MPC can reduce the electricity drawn from the grid under various conditions such that in the cases investigated in this work, an improvement of up to 12.14 % compared to the rule-based controller was achieved, while even in the worst case, an improvement of 3.93 % was achieved. However, it was shown that the PV energy, electricity demand, and typical periods greatly impacted the results. Furthermore, it was shown that the improvements to be gained depend on the environmental conditions, such that investigations for various weather conditions are necessary to evaluate the performance of a model predictive control approach for this hybrid battery-hydrogen energy storage

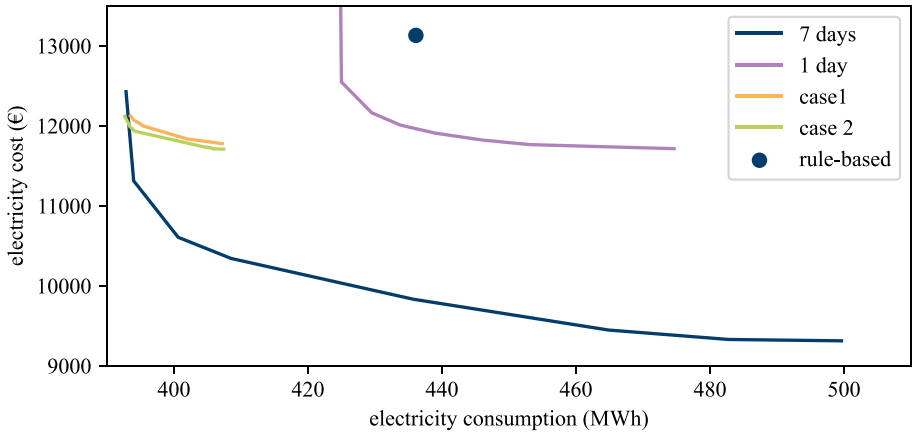

Fig. 21. Visualization of the Pareto front for runs of the MPC framework compared to runs of the MPC framework with a 1-day and a 7-day prediction horizon with a 24-h control horizon shown in Fig. 19. Case 1 is a run of the MPC framework with a prediction horizon of 2 days with a price forecast of 1 day, and case 2 is a run of the MPC framework with a prediction horizon of 4 days with a price for.ecast of 1 day.

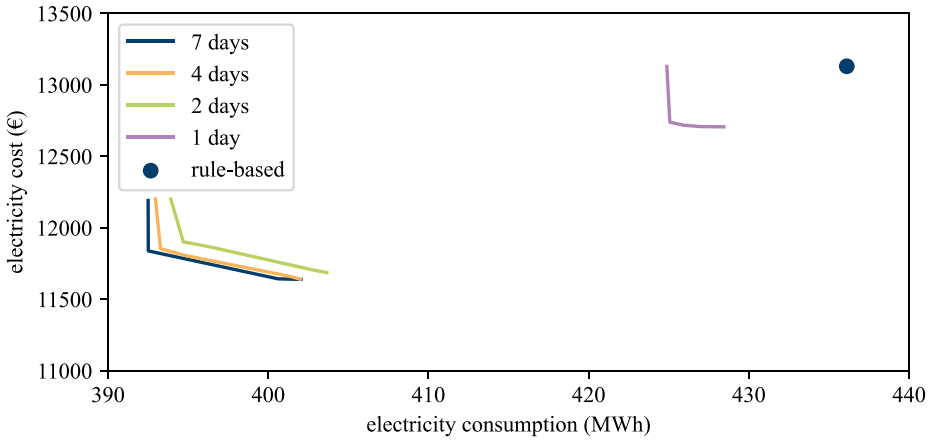

Fig. 22. Visualization of the Pareto front for runs of the MPC framework with different prediction horizons and a control horizon of 24 h for a three-tier time-of-use concept.

system. In future works, the impact of the typical periods on the results could be investigated in more detail.

Moreover, the impact of a minimal operational time and varying electricity prices on the results of the MPC framework are investigated. The consideration of a minimum operational time for the fuel cell and the electrolyzer was shown to have only a minor impact on the performance of the MPC framework while decreasing the overall number of start-ups and shut-downs by 29.62 %. An economic optimization considering a variable grid price results in a steep decrease of the operational cost of up to 47 % for the considered typical weeks in comparison to a rule-based controller if the price curves of the next seven days are available. In more realistic scenarios with an accurate price forecast of just one day, the electricity cost is reduced by 11 %, while the use of a three-tier time-of-use concept leads to an 11.3% reduction in the electricity cost for the considered typical weeks. Finally, the Pareto fronts of multi-objective optimizations considering the grid electricity consumption and a variable grid price are investigated. It was shown that MPC can be utilized to reduce the electricity cost drastically while decreasing the electricity consumption in all cases. Furthermore, the impact of the prediction and control horizon on the Pareto optimal solution was investigated. The results show that increasing the prediction horizon above one day increased the performance of the model predictive controller, while increases above a two-day horizon improved the performance only slightly.

In conclusion, this paper presents a framework for validating different operational strategies and settings for model predictive control algorithms. The potential effectiveness of MPC is investigated utilizing perfect foresight and a detailed simulation model. MPC can reduce the operational cost while decreasing the electricity consumption for the investigated hybrid battery-hydrogen energy storage system under all circumstances that were considered in this work.

Declaration of Competing Interest

The authors declare that they have no known competing financial interests or personal relationships that could have appeared to influence the work reported in this paper.

Data availability

Data will be made available on request.

Acknowledgment

Funding: This work was supported by the German Federal Ministry of Education and Research, [Grant No. 03SF0573]

References

[1] Umweltbundesamt, Erneuerbare Energien in Deutschland 2020: Daten zur Entwicklung im Jahr 2020, 2021.
[2] Brouwer AS, van den Broek M, Zappa W, Turkenburg WC, Faaij A. Least-cost options for integrating intermittent renewables in low-carbon power systems. Applied Energy 2016;161:48–74. https://doi.org/10.1016/j.apenergy.2015.09.090. ISSN 03062619.
[3] Gabrielli P, Gazzani M, Martelli E, Mazzotti M. Optimal design of multi-energy systems with seasonal storage. Applied Energy 2018;219:408–24. https://doi.org/10.1016/j.apenergy.2017.07.142. ISSN 03062619.
[4] Brey JJ. Use of hydrogen as a seasonal energy storage system to manage renewable power deployment in Spain by 2030. International Journal of Hydrogen Energy 2021;46(33):17447–57. https://doi.org/10.1016/j.ijhydene.2020.04.089. ISSN 03603199.
[5] Le TS, Nguyen TN, Bui D-K, Ngo TD. Optimal sizing of renewable energy storage: A techno-economic analysis of hydrogen, battery and hybrid systems considering degradation and seasonal storage. Applied Energy 2023;336:120817. https://doi.org/10.1016/j.apenergy.2023.120817. ISSN 03062619.
[6] Olatomiwa L, Mekhilef S, Ismail MS, Moghavvemi M. Energy management strategies in hybrid renewable energy systems: A review. Renewable and Sustainable Energy Reviews 2016;62:821–35. https://doi.org/10.1016/j.rser.2016.05.040. ISSN 13640321.
[7] Van LP, Chi KD, Duc TN. Review of hydrogen technologies based microgrid: Energy management systems, challenges and future recommendations. International Journal of Hydrogen Energy 2023;48(38):14127–48. https://doi.org/10.1016/j.ijhydene.2022.12.345. ISSN 03603199.
[8] Abdelghany MB, Mariani V, Liuzza D, Glielmo L. Hierarchical model predictive control for islanded and grid-connected microgrids with wind generation and hydrogen energy storage systems. International Journal of Hydrogen Energy 2024;51:595–610. https://doi.org/10.1016/j.ijhydene.2023.08.056. ISSN 03603199.
[9] M. Korpaas, R. Hildrum, A. T. Holen, M. Korpaas, R. Hildrum, A. T. Holen, Optimal operation of hydrogen storage for energy sources with stochastic input, in: 2003 IEEE Bologna Power Tech Conference Proceedings, vol. 4, 8–pp, 2003, DOI: 10.1109/PTC.2003.1304706.
[10] Cau G, Cocco D, Petrollese M, Knudsen Kær S, Milan C. Energy management strategy based on short-term generation scheduling for a renewable microgrid using a hydrogen storage system. Energy Conversion and Management 2014;87:820–31. https://doi.org/10.1016/j.enconman.2014.07.078. ISSN 01968904.
[11] Valverde L, Bordons C, Rosa F. Integration of Fuel Cell Technologies in Renewable-Energy-Based Microgrids Optimizing Operational Costs and Durability. IEEE Transactions on Industrial Electronics 2016;63(1):167–77. https://doi.org/10.1109/TIE.2015.2465355. ISSN 0278-0046.
[12] Daneshvar M, Mohammadi-Ivatloo B, Zare K, Asadi S. Transactive energy management for optimal scheduling of interconnected microgrids with hydrogen energy storage. International Journal of Hydrogen Energy 2021;46(30):16267–78. https://doi.org/10.1016/j.ijhydene.2020.09.064. ISSN 03603199.
[13] Gbadega PA, Saha AK. Impact of Incorporating Disturbance Prediction on the Performance of Energy Management Systems in Micro-Grid. IEEE Access 2020;8:162855–79. https://doi.org/10.1109/ACCESS.2020.3021598.
[14] Huang C, Zong Y, You S, Træholt C, Zheng Y, Wang J, Zheng Z, Xiao X. Economic and resilient operation of hydrogen-based microgrids: An improved MPC-based optimal scheduling scheme considering security constraints of hydrogen facilities. Applied Energy 2023;335:120762. https://doi.org/10.1016/j.apenergy.2023.120762. ISSN 03062619.
[15] Modu B, Abdullah MP, Bukar AL, Hamza MF. A systematic review of hybrid renewable energy systems with hydrogen storage: Sizing, optimization, and energy management strategy. International Journal of Hydrogen Energy 2023;48(97):38354–73. https://doi.org/10.1016/j.ijhydene.2023.06.126. ISSN 03603199.

[16] Bordons C, Garcia-Torres F, Ridao MA. Model Predictive Control of Microgrids. Cham: Springer International Publishing; 2020. https://doi.org/10.1007/978-3-030-24570-2. ISBN 978-3-030-24569-6.
[17] Modu B, Abdullah MP, Bukar AL, Hamza MF, Adewolu MS. Energy management and capacity planning of photovoltaic-wind-biomass energy system considering hydrogen-battery storage. Journal of Energy Storage 2023;73:109294. https://doi.org/10.1016/j.est.2023.109294. ISSN 2352152X.
[18] Li Z, Liu Y, Du M, Cheng Y, Shi Le. Modeling and multi-objective optimization of a stand-alone photovoltaic-wind turbine-hydrogen-battery hybrid energy system based on hysteresis band. International Journal of Hydrogen Energy 2023;48(22):7959–74. https://doi.org/10.1016/j.ijhydene.2022.11.196. ISSN 03603199.
[19] Šimunović J, Radica G, Barbir F. The effect of components capacity loss on the performance of a hybrid PV/wind/battery/hydrogen stand-alone energy system. Energy Conversion and Management 2023;291:117314. https://doi.org/10.1016/j.enconman.2023.117314. ISSN 01968904.
[20] Alili H, Mahmoudimehr J. Techno-economic assessment of integrating hydrogen energy storage technology with hybrid photovoltaic/pumped storage hydropower energy system. Energy Conversion and Management 2023;294:117437. https://doi.org/10.1016/j.enconman.2023.117437. ISSN 01968904.
[21] Clarke WC, Brear MJ, Manzie C. Control of an isolated microgrid using hierarchical economic model predictive control. Applied Energy 2020;280:115960. https://doi.org/10.1016/j.apenergy.2020.115960. ISSN 03062619.
[22] Gonzalez-Rivera E, Garcia-Trivino P, Sarrias-Mena R, Torreglosa JP, Jurado F, Fernandez-Ramirez LM. Model Predictive Control-Based Optimized Operation of a Hybrid Charging Station for Electric Vehicles. IEEE Access 2021;9:115766–76. https://doi.org/10.1109/ACCESS.2021.3106145.
[23] Yassuda Yamashita D, Vechiu I, Gaubert J-P. Two-level hierarchical model predictive control with an optimised cost function for energy management in building microgrids. Applied Energy 2021;285:116420. https://doi.org/10.1016/j.apenergy.2020.116420. ISSN 03062619.
[24] Li J, Zou W, Yang Q, Bao H. Towards net-zero smart system: An power synergy management approach of hydrogen and battery hybrid system with hydrogen safety consideration. Energy Conversion and Management 2022;263:115717. https://doi.org/10.1016/j.enconman.2022.115717. ISSN 01968904.
[25] Kumar K, Bae S. Two-layer energy management strategy for renewable power-to-gas system-based microgrids. Journal of Energy Storage 2023;61:106723. https://doi.org/10.1016/j.est.2023.106723. ISSN 2352152X.
[26] Thaler B, Posch S, Wimmer A, Pirker G. Hybrid model predictive control of renewable microgrids and seasonal hydrogen storage. International Journal of Hydrogen Energy 2023;48(97):38125–42. https://doi.org/10.1016/j.ijhydene.2023.06.067. ISSN 03603199.
[27] Shahzad S, Abbasi MA, Chaudhry MA, Hussain MM. Model Predictive Control Strategies in Microgrids: A Concise Revisit. IEEE Access 2022;10:122211–25. https://doi.org/10.1109/ACCESS.2022.3223298.
[28] Garcia-Torres F, Bordons C. Optimal Economical Schedule of Hydrogen-Based Microgrids With Hybrid Storage Using Model Predictive Control. IEEE Transactions on Industrial Electronics 2015;62(8):5195–207. https://doi.org/10.1109/TIE.2015.2412524. ISSN 0278-0046.
[29] Kotzur L, Nolting L, Hoffmann M, Groß T, Smolenko A, Priesmann J, Büsing H, Beer R, Kullmann F, Singh B, Praktiknjo A, Stolten D, Robinius M. A modeler's guide to handle complexity in energy systems optimization. Advances in Applied Energy 2021;4:100063. https://doi.org/10.1016/j.adapen.2021.100063. ISSN 26667924.
[30] Abdelghany MB, Shehzad MF, Liuzza D, Mariani V, Glielmo L. Optimal operations for hydrogen-based energy storage systems in wind farms via model predictive control. International Journal of Hydrogen Energy 2021;46(57):29297–313. https://doi.org/10.1016/j.ijhydene.2021.01.064. ISSN 03603199.
[31] Abdelghany MB, Al-Durra A, Zeineldin H, Gao F. Integrating scenario-based stochastic-model predictive control and load forecasting for energy management of grid-connected hybrid energy storage systems. International Journal of Hydrogen Energy 2023;48(91):35624–38. https://doi.org/10.1016/j.ijhydene.2023.05.249. ISSN 03603199.
[32] Shen W, Zeng B, Zeng M. Multi-timescale rolling optimization dispatch method for integrated energy system with hybrid energy storage system. Energy 2023;283:129006. https://doi.org/10.1016/j.energy.2023.129006. ISSN 03605442.
[33] Cardona P, Costa-Castelló R, Roda V, Carroquino J, Valiño L, Serra M. Model predictive control of an on-site green hydrogen production and refuelling station. International Journal of Hydrogen Energy 2023;48(47):17995–8010. https://doi.org/10.1016/j.ijhydene.2023.01.191. ISSN 03603199.
[34] A. Senkel, C. Bode, J.-P. Heckel, O. Schülting, G. Schmitz, C. Becker, A. Kather, Status of the TransiEnt Library: Transient Simulation of Complex Integrated Energy Systems, in: Proceedings of 14th Modelica Conference 2021, Linköping, Sweden, September 20–24, 2021, Linköping Electronic Conference Proceedings, Linköping University Electronic Press, 187–196, 2021, DOI: 10.3384/ecp21181187.
[35] Andresen L, Bode C, Schmitz G. Dynamic simulation of different transport options of renewable hydrogen to a refinery in a coupled energy system approach. International Journal of Hydrogen Energy 2018;43(42):19600–14. https://doi.org/10.1016/j.ijhydene.2018.08.111. ISSN 03603199.
[36] Buttler A, Spliethoff H. Current status of water electrolysis for energy storage, grid balancing and sector coupling via power-to-gas and power-to-liquids: A review. Renewable and Sustainable Energy Reviews 2018;82:2440–54. https://doi.org/10.1016/j.rser.2017.09.003. ISSN 13640321.
[37] Petkov I, Gabrielli P. Power-to-hydrogen as seasonal energy storage: an uncertainty analysis for optimal design of low-carbon multi-energy systems. Applied Energy 2020;274(3):115197. https://doi.org/10.1016/j.apenergy.2020.115197. ISSN 03062619.
[38] Wetter M, Zuo W, Nouidui TS, Pang X. Modelica Buildings library. Journal of Building Performance Simulation 2014;7(4):253–70. https://doi.org/10.1080/19401493.2013.765506. ISSN 1940-1493.
[39] Riedl SM. Development of a Hydrogen Refueling Station Design Tool. International Journal of Hydrogen Energy 2020;45(1):1–9. https://doi.org/10.1016/j.ijhydene.2019.09.234. ISSN 03603199.
[40] Trifkovic M, Sheikhzadeh M, Nigim K, Daoutidis P. Modeling and Control of a Renewable Hybrid Energy System With Hydrogen Storage. IEEE Transactions on Control Systems Technology 2014;22(1):169–79. https://doi.org/10.1109/TCST.2013.2248156. ISSN 1063-6536.
[41] Scheepers F, Stähler M, Stähler A, Rauls E, Müller M, Carmo M, Lehnert W. Improving the Efficiency of PEM Electrolyzers through Membrane-Specific Pressure Optimization. Energies 2020;13(3):612. https://doi.org/10.3390/en13030612.
[42] E. Tzimas, C. Filiou, S. D. Peteves, J.-B. Veyret, et al., Hydrogen storage: state-of-the-art and future perspective, EU Commission, JRC Petten, EUR 20995EN (2003).
[43] W. F. Holmgren, C. W. Hansen, M. A. Mikofski, pvlib python: a python package for modeling solar energy systems, Journal of Open Source Software 3 (29) (2018) 884, 10.21105/joss.00884.
[44] Deutscher Wetterdienst, Open Data, https://www.dwd.de/DE/leistungen/, (accessed 19.01.2024), 2024.
[45] Benigni A, Xhonneux A, Carta D, Pesch T, Muller D. On the development of control solutions for local energy communities, at-Automatisierungstechnik 2022;70(12):1095–115.
[46] A. Holtwerth, A. Xhonneux, D. Müller, Data-Driven Generation of Mixed-Integer Linear Programming Formulations for Model Predictive Control of Hybrid Energy Storage Systems using detailed nonlinear Simulation Models, in: OSMSES 2022: 1st International Workshop on Open Source Modelling and Simulation of Energy Systems, 2022.
[47] C. F. Jekel, G. Venter, pwlf: A Python Library for Fitting 1D Continuous Piecewise Linear Functions, 10.13140/RG.2.2.28530.56007, URL: https://github.com/cjekel/piecewise_linear_fit_py, (accessed 10.01.2024), 2019.
[48] Kämper A, Holtwerth A, Leenders L, Bardow A. AutoMoG 3D: Automated Data-Driven Model Generation of Multi-Energy Systems Using Hinging Hyperplanes. Frontiers in Energy Research 2021;9:716. https://doi.org/10.3389/fenrg.2021.719658.
[49] Vielma JP, Ahmed S, Nemhauser G. Mixed-Integer Models for Nonseparable Piecewise-Linear Optimization: Unifying Framework and Extensions. Operations Research 2010;58(2):303–15. https://doi.org/10.1287/opre.1090.0721. ISSN 0030-364X.
[50] Langiu M, Shu DY, Baader FJ, Hering D, Bau U, Xhonneux A, Müller D, Bardow A, Mitsos A, Dahmen M. COMANDO: A Next-Generation Open-Source Framework for Energy Systems Optimization. Computers & Chemical Engineering 2021;152(11):107366. https://doi.org/10.1016/j.compchemeng.2021.107366. ISSN 00981354.
[51] Systemes Dassault, FMPy, https://fmpy.readthedocs.io/en/latest, (accessed 10.01.2024), 2024.
[52] F. Fan, R. Zhang, Y. Xu, Robustly coordinated operation of an emission-free microgrid with hybrid hydrogen-battery energy storage, CSEE Journal of Power and Energy Systems, 10.17775/CSEEJPES.2021.04200, ISSN 20960042.
[53] Hoffmann M, Priesmann J, Nolting L, Praktiknjo A, Kotzur L, Stolten D. Typical periods or typical time steps? A multi-model analysis to determine the optimal temporal aggregation for energy system models. Applied Energy 2021;304(7):117825. https://doi.org/10.1016/j.apenergy.2021.117825. ISSN 03062619.
[54] Kotzur L, Markewitz P, Robinius M, Stolten D. Time series aggregation for energy system design: Modeling seasonal storage. Applied Energy 2018;213:123–35. https://doi.org/10.1016/j.apenergy.2018.01.023. ISSN 03062619.
[55] L. L. Gurobi Optimization, Gurobi Optimizer Reference Manual. URL: https://www.gurobi.com (accessed 19.01.2024), 2024.
[56] Stute J, Kühnbach M. Dynamic pricing and the flexible consumer – Investigating grid and financial implications: A case study for Germany. Energy Strategy Reviews 2023;45:100987. https://doi.org/10.1016/j.esr.2022.100987. ISSN 2211467X.
[57] C. Jia, J. Cui, W. Qiao, L. Qu, A Reduced-Scale Power Hardware-in-the-Loop Platform for Fuel Cell Electric Vehicles, in: 2021 IEEE Transportation Electrification Conference & Expo (ITEC), IEEE, 370–375, ISBN 978-1-7281-7583-6, 2021, DOI: 10.1109/ITEC51675.2021.9490118.